High-fidelity delivery of kilowatt-level single-mode laser through tapered multimode fiber over a hundred meters

Xiao Chen[1,7], Shanmin Huang[1,7], Liangjin Huang[1,2,3,4], Zhiping Yan[1,2,3], Zhiyong Pan[1,2,3,5], Zongfu Jiang[1,2,3], and Pu Zhou[1,2,3,6]

[1] *College of Advanced Interdisciplinary Studies, National University of Defense Technology, Changsha 410073, China*

[2] *Nanhu Laser Laboratory, National University of Defense Technology, Changsha 410073, China*

[3] *Hunan Provincial Key Laboratory of High Energy Laser Technology, National University of Defense Technology, Changsha 410073, China*

[4] *huangliangjin203@163.com*

[5] *panzy168@163.com*

[6] *zhoupu203@163.com*

[7] *These authors contributed equally to this work*

Abstract The immediate priorities for high-power delivery employing solid-core fibers are balancing the nonlinear effect and beam deterioration. Here, the scheme of tapered multimode fiber is experimentally realized. The tapered multimode fiber, featuring a 15 m (24/200 μm)-10 m (tapered region)-80 m (48/400 μm) profile, guides the laser with a weakly coupled condition. With the input power of 1035 W, the maximum output

This peer-reviewed article has been accepted for publication but not yet copyedited or typeset, and so may be subject to change during the production process. The article is considered published and may be cited using its DOI.

10.1017/hpl.2024.91

power over the 105-meter delivery is 962 W, corresponding to a high efficiency of over 93% and a nonlinear suppression ratio of over 50 dB. Mode resolving results show high-order-mode contents of less than -30 dB in the whole delivery path, resulting in a high-fidelity delivery with the M^2 factors of 1.20 and 1.23 for the input and output lasers, respectively. Furthermore, the ultimate limits of delivery lengths for solid-core weakly coupled fibers are discussed. This work provides a valuable reference to reconsider the future boom of high-power laser delivery based on solid-core fibers.

Key words: Tapered multimode fiber, Laser delivery, Single mode, Nonlinear effect, Hundred meters.

I. INTRODUCTION

High-power single-mode laser delivery has become a renewed interest recently [1-4], due to its potential applications in extreme manufacturing, precise welding, and the defense industry [5]. Solid-core delivery fibers offer a brilliant solution for high-power delivery, and this success is driven by the integrated compact for flexible operation and robust laser confinement. At present, many scenarios spawn a compound demand for high-power, single-mode, and long-distance delivery, for instance, the application of precise welding needs a single-mode beam to promote working efficiency and simultaneously a long-distance delivery to expand the processing range.

The existing solid-core fiber-based laser delivery system has a technical bottleneck in that the power, beam quality, and nonlinear threshold cannot be balanced. For single-mode laser operating at several kilowatts, the main obstacles impeding the long-

https://doi.org/10.1017/hpl.2024.91 Published online by Cambridge University Press

distance delivery are nonlinear effects and beam quality degradation. For industrial fiber lasers with a broadband spectrum, the dominant nonlinear effect is stimulated Raman scattering (SRS) [6, 7]. To increase the delivery distance, extended-mode-area (EMA) fibers with enhanced nonlinear thresholds are needed. However, multimode operation in the large core diameter accelerates the degradation of beam quality in the whole delivery path. Although the research in single-mode laser sources has pushed the power record to the order of several kilowatts [8] and even 10 kW [9], the results with a long-distance single-mode delivery over more than tens of meters [4, 10] are far behind, which severely limits the performance of laser beam reaching the workbench. To handle this bottleneck, the key is seeking a bilateral solution for preserving high-fidelity transmission and improving the nonlinear threshold.

An effective strategy is developing special fibers with increased high-order-mode (HOM) losses, which has led to multiple fiber designs [11-13], including modified clad profiles or microstructure fibers. A variety of designs, such as single-trench fiber [14, 15], chirally-coupled-core fiber [16], and all-solid photonic bandgap fiber [17], have seen stages of success in surpassing conventional fibers. A higher HOM loss extends the possibility of enlarging the core diameter, yielding a robust single-mode operation and a higher power scalability. However, it is a general fact that these special fibers suffer from more complex preparation processes, more stringent manufacturing tolerances, and limited impracticality for integration. Owing to the greater bending sensitivity, the future boom for them is more likely to obtain gain fibers with moderate lengths rather than long-distance delivery fibers. Hence, more efforts should be

https://doi.org/10.1017/hpl.2024.91 Published online by Cambridge University Press

afforded to facilitate their applications, especially compact integrations with conventional fibers [18]. Recent research has demonstrated the integration potential of a solid-core microstructure fiber with a conventional fiber, which enables a 10 kW laser delivery of over 30 m [19].

Recently, hollow-core fiber (HCF) has become a rising star in the field of single-mode and long-distance delivery [1, 3, 20, 21]. HCFs offer unprecedented advantages of low nonlinearity, excellent single-mode property, and high damage threshold, which makes them a highly attractive option for the long-distance delivery of high-brightness laser beams. Moreover, the loss record of HCFs is refreshed rapidly in recent years, and the latest records achieved by HCFs presented us comparable loss values than conventional fibers covering broadband spectrum regions [22, 23]. Up to now, the record-breaking delivery length has been confirmed in multiple wavebands, ranging from the conventional 1 μm waveband (1000 m) [1] to mid-infrared (108 m) [24] and visible (300 m) [25] regions. These results simultaneously validate the power handling capacity of HCFs above kilowatts for both continuous and pulsed laser regimes. HCFs create an air-based environment to facilitate the nonlinear-effect-free delivery of high-power laser, the future attempts should be focused on realizing compact and highly efficient integrations with the current laser systems. However, all the high-power delivery results are carried out based on the spatially coupled architectures currently, which suffer from thermally induced focusing shifts at different power levels. Hence, the stability is limited, and discontinuous adjustments are required during the power scaling process.

https://doi.org/10.1017/hpl.2024.91 Published online by Cambridge University Press

Another strategy is controlling the mode coupling in conventional fibers while enlarging the core diameters, which gives birth to the weakly coupled fiber [26]. With the weakly coupled condition, fiber modes propagate along the long-distance path with high fidelity, and the adjacent modes have negligible mode coupling coefficients. The mode coupling between the fundamental mode and the HOMs obeys the field coupling equation, in which the phase matching condition is strongly correlated to the propagation constant (β) difference. In other words, a weakly coupled condition, represented by a large β difference, means a large index difference Δn_{eff} between adjacent modes. Therefore, the high-fidelity delivery of conventional fiber should consider a tradeoff between the maximum core diameter and the numerical aperture (NA) [4]. The investigations of weakly coupled fiber date back to 1998, in which Fermann reported the preservation of the fundamental mode with a core diameter of 45 μm and emphasized the beneficial effect of a larger cladding diameter [27]. Since then, high beam quality outputs have been experimentally demonstrated in 100 μm to 400 μm core diameters [28, 29]. The remarkable advances in 2014 and 2019 showed great examples in balancing the core diameter and NA for weakly coupled delivery, resulting in an 800 W, 100 m delivery in the 30 μm fiber and a 1000 W, 100 m delivery in the 60 μm fiber. In these investigations, a key procedure is the dominated excitation of the fundamental mode, for example, employing a cascade mode field adapter [4]. However, as a kind of fiber device, the mode field adapter has limited power handling ability and suffers from inescapable mode degradation due to intrinsic defects during fabrication [30, 31].

https://doi.org/10.1017/hpl.2024.91 Published online by Cambridge University Press

The immediate priorities are looking for solutions for the two key issues: (1) How to improve the nonlinear threshold of long-distance delivery? (2) How to achieve a high-fidelity delivery by optimizing the launching condition and preventing transmission deterioration? In this work, the solution of tapered multimode fiber is proposed. We attempt to push the delivery of kilowatt-level, single-mode laser to over a hundred meters based on a monolithic, solid-core, weakly coupled, and tapered multimode fiber, featuring a high-fidelity delivery without beam quality deterioration. In Section 2, the design principle of multimode tapered fiber and the fabrication results are presented. In Section 3, the high-fidelity delivery of a kilowatt-level single-mode laser is experimentally demonstrated. The results show a high transmission efficiency of over 93%, a high signal-to-SRS ratio of over 50 dB, and a high-fidelity delivery with negligible beam degradation. In Section 4, the ultimate limits of delivery length for the sing-mode laser with different powers are discussed for reference.

II. WEAKLY COUPLED FIBER AND FIBER FABRICATION

The high-fidelity transmission of a single-mode laser means that the fundamental mode remains isolated from the HOMs, preventing possible energy exchange between them. In an ideal multimode fiber, the eigenmodes are intrinsically orthogonal and propagate through independent channels. Nevertheless, unexpected perturbations within actual fibers, such as slight fluctuations in refractive index or geometric dimensions, and bending distortion, can impact the mode isolation. In this way, owing to the uniform perturbation of the local dielectric constant, the fundamental mode and the HOMs are easily coupled to each other over a long-distance delivery. The strength of mode

https://doi.org/10.1017/hpl.2024.91 Published online by Cambridge University Press

coupling between modes is determined by the phase matching condition, which is related to the propagation constant difference of modes. Generally, the strength of mode coupling between adjacent modes is dominant, and a larger mode spacing results in a decreased mode coupling. Hence, the key issue for the high-fidelity delivery of single-mode laser is increasing mode spacing between the fundamental mode and the LP_{11} mode. The coupled mode equations for the two modes are written as [32]:

$$\begin{cases} \dfrac{\mathrm{d}A_1}{\mathrm{d}z} = iK_{11}A_1 + iK_{12}A_2 \exp\left[i\left(\beta_2 - \beta_1\right)z\right] \\ \dfrac{\mathrm{d}A_2}{\mathrm{d}z} = iK_{22}A_2 + iK_{21}A_1 \exp\left[i\left(\beta_1 - \beta_2\right)z\right] \end{cases} \tag{1}$$

where A_1 and A_2 are the amplitudes of two modes, β_1 and β_2 are the propagation constants of two modes, and the coupling efficiencies K_{12} and K_{21} obey the symmetry relation $K_{12} = K_{21}$.

According to the coupled mode equations, a phase matching condition should be fulfilled to allow sufficient mode coupling. This means that the strength of mode coupling could be reduced by enlarging the propagation constant difference $\Delta\beta$ or effective index difference Δn_{eff} between modes. Therefore, one can conclude that it might be appropriate to employ weakly coupled multimode fibers with a high effective index difference instead of single-mode fibers to transport a single-mode beam. From the birefringence of commercially available polarization-maintaining fibers, it can be deduced that the polarization mode coupling is efficiently suppressed when the effective index difference Δn_{eff} between adjacent modes is larger than 5×10^{-4}. Furthermore, J.M. Fini and S. Ramachandran stated that the reference value to meet the weakly coupled condition could be limited to the target [33, 34]:

https://doi.org/10.1017/hpl.2024.91 Published online by Cambridge University Press

$$\Delta n_{eff} > 1\times10^{-4} \quad (2)$$

To achieve the weakly coupled condition, both a large refractive index contrast between the core and the cladding and a small core diameter are needed [35]. However, a small core diameter reduces the effective mode area, which accelerates the nonlinearities for long-distance delivery. Here, a tradeoff among the core diameter, NA, and Δn_{eff} between the fundamental mode and the LP_{11} mode is calculated. According to the results in Fig. 1(a), the Δn_{eff} shows an inverse proportion relationship with the core diameter. A higher value of NA induces a larger Δn_{eff}, corresponding to a better weakly coupled condition. However, for the core diameters across 40 μm, the Δn_{eff} and NA have less correlation for a fixed core diameter. This phenomenon restricts further scaling of core diameter to satisfy the weakly coupled condition even with a large NA value. Based on the principle defined in equation (2), the maximum core diameter obeying the weakly coupled condition is confined to nearly 50~60 μm. This principle will guide the design of the tapered multimode fiber drawn in this work.

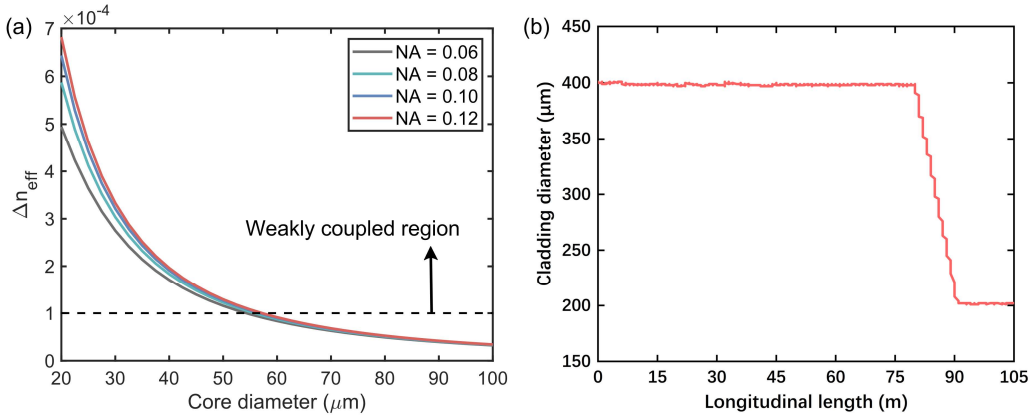

Fig. 1 (a) The calculated results of effective index differences with different fiber parameters. (b) The measured fiber dimension profile of the tapered multimode fiber.

https://doi.org/10.1017/hpl.2024.91 Published online by Cambridge University Press

Subsequently, the tapered multimode fiber is drawn adiabatically by using the fiber drawing tower, and the measured fiber dimension profile along the longitudinal direction is plotted in Fig. 1(b). As shown in Fig. 2(a), the core/clad dimensions at the thin and thick ends are nearly 24/200 μm and 48/400 μm, respectively. The effective mode areas at the thin and thick ends are calculated to be 347 μm^2 and 1089 μm^2, respectively. The total fiber length is 105 m, comprising a thick region of 80 m, a tapered region of 10 m, and a thin region of 15 m. The measured refractive index profile is shown in Fig. 2(b), and the NA is early ~0.06. The cut-back test indicates a core attenuation of ~3.5 dB/km at the signal wavelength (1080 nm), which guarantees a relatively high efficiency (>90%) for the delivery application of over a hundred meters.

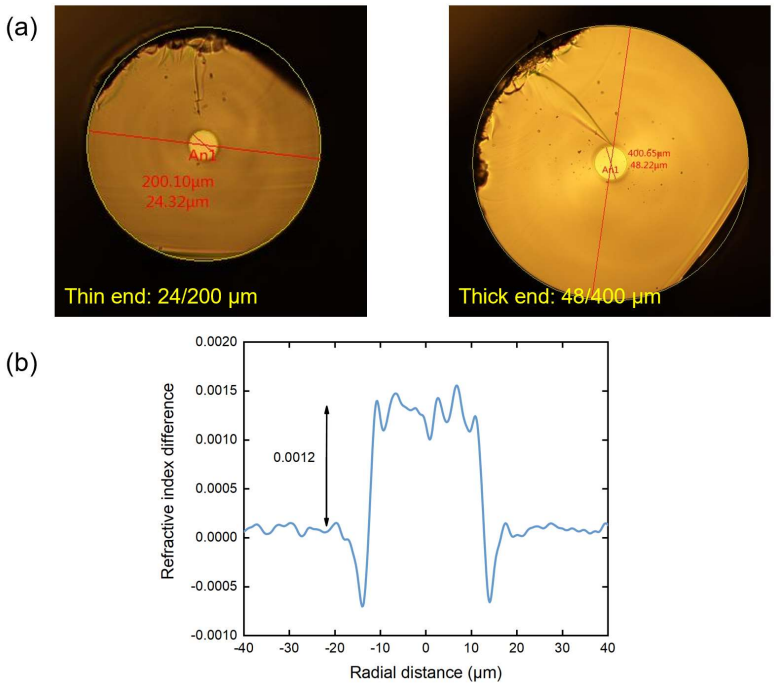

Fig. 2 The geometric and refractive descriptions of of the tapered fiber. (a) Geometric dimensions at both ends. (b) Measured refractive index profile

https://doi.org/10.1017/hpl.2024.91 Published online by Cambridge University Press

The profile of the tapered fiber is designed by considering the balance among the weakly coupled condition, mode matching with the laser source, and the nonlinear suppression. At the thin end, the mode matching between the tapered fiber and the output fiber of the laser source should be considered. The core/cladding ratio of the tapered fiber results in a few possible specifications for the thin end, e.g., 20/167 μm, 24/200 μm, or 30/250 μm. The output fiber of the laser source has a dimension of 20/250 μm. Hence, compared with 30/250 μm, the dimension of 24/200 μm is more favorable to achieve mode matching with the output fiber of the laser source. To prevent mode degradation over a long delivery path, the maximum core diameter at the thick end should obey the weakly coupled condition. Based on the principle defined by $\Delta n_{eff} > 1\times10^{-4}$, the maximum core diameter obeying the weakly coupled condition is confined to nearly 50~60 μm. For a moderate and secure consideration, the core diameter at the thick end is limited to below 50 μm, this is a moderate value to realize a large mode area and a high-fidelity transmission. Therefore, based on these considerations, the profile of 24/200 μm and 48/400 μm is selected finally.

Through the repeat fiber drawing experiments, the optimized interval from nearly 8 m to 12 m for achieving a uniformly shrinkable taper is found. Hence, a moderate length of 10 m for the tapered region is selected for achieving a uniformly shrinkable taper (from 48/400 μm to 24/200 μm), which is vital for mode preservation. To enhance the nonlinear threshold, the thick end should dominate the entire length of the tapered delivery fiber. In addition, to reach the goal of high-power laser delivery over 100 m, the length total length of the thin and thick ends should be longer than 90 m (considering

https://doi.org/10.1017/hpl.2024.91 Published online by Cambridge University Press

the taper length of 10 m). Hence, the ultimate design is determining the respective lengths of the thin and thick ends. There are a few optional schemes, for instance, (a) 5 m (thin end) and 90 m (thick end), (b) 10 m (thin end) and 85 m (thick end), or (c) 15 m (thin end) and 80 m (thick end), etc. It is a clear fact that the effective mode area of the tapered fiber increases gradually from schemes (a)-(c), which means stronger SRS suppression. Therefore, if scheme (c) can realize a high-quality (signal-to-SRS ratio of over 50 dB) delivery over 100 m, schemes (a) and (b) will undoubtedly be even better.

III. EXPERIMENTAL RESULTS AND SIMULATIONS

The experimental setup for high-power delivery is shown in Fig. 3(a), in which a monolithic fiber oscillator with an output power of over 1 kW and a 20/250 μm output fiber is employed as the laser source. This source operates at a signal wavelength of 1080 nm and has pure spectra at the whole power trace, i.e., no SRS effect is observed. The 20/250 μm output fiber is optimally spliced with the thin end (i.e., 24/200 μm) of the tapered multimode fiber, the splicing optimization is instructed by Ref. [36]. After splicing, the excited HOM contents in the whole delivery path are measured to be below -30 dB (the result will be presented in Fig. 7), which ensures a high-fidelity delivery of the emitted laser beam from the 20/250 μm output fiber to the whole delivery path. To avoid unexpected mode coupling induced by macro-bending, the tapered multimode fiber is loosely coiled with a 60 cm diameter. At the output end, a power meter, an optical spectrum analyzer, and a beam quality analyzer are used for the laser beam characterization. The main power of the laser beam is transferred to the power meter through a high-transmittance (HT) mirror, and the sampled beam is directed by a high-

https://doi.org/10.1017/hpl.2024.91 Published online by Cambridge University Press

reflectivity (HR) mirror. The trace of output power is plotted in Fig. 3(b), which presents a linear correlation between the input and output power. The maximum output power is 962 W when the input laser is 1035 W. In the whole power trace, the transmission efficiency keeps a stable value of nearly 93%. This efficiency is mainly limited by the attenuation of optical fiber, which could be further improved by increasing the NA.

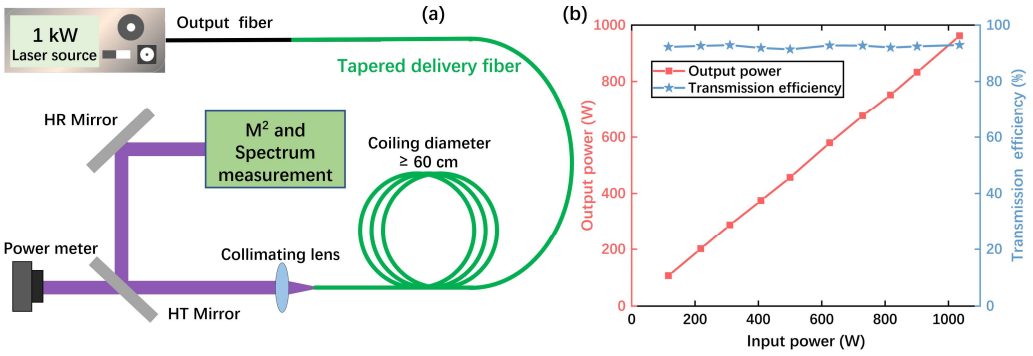

Fig. 3 (a) Experimental setup for high-power delivery. (b) Relationship between the input and output power, and the total transmission efficiency.

The recorded spectra at different output powers are illustrated in Fig. 4(a). At the highest output power, the signal-to-SRS ratio is over 50 dB, demonstrating the ideal suppression of the nonlinear effect after the whole delivery path of 105 m. To evaluate the mode fidelity after delivery, the beam quality M^2 factors of the input and output laser are recorded for comparison, as shown in Fig. 4(b). The input M^2 factor represents the beam quality of the laser source emitting from the 20/250 μm output fiber. As can be seen, the input and output M^2 factors remain stable values at nearly 1.20 and 1.23, respectively, indicating superior mode fidelity in the whole delivery path. The current results feature almost negligible beam quality degradation and demonstrate the

https://doi.org/10.1017/hpl.2024.91 Published online by Cambridge University Press

excellent structure of the tapered fiber profile for mode preservation. The high-fidelity delivery reported here should be attributed to the following factors: (1) the optimum mode launching at the splicing point of the 20/250 μm output fiber and the thin end of the tapered fiber; (2) the weakly coupled mechanism of tapered multimode fiber by balancing the core diameter and NA; (3) the excellent taper profile formed by fiber drawing.

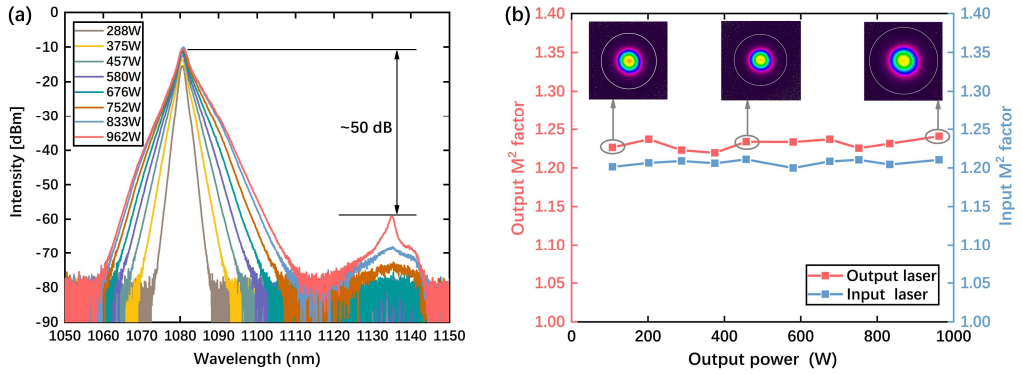

Fig. 4 (a) The recorded spectra at different output powers. (b) The beam quality M^2 factors of the input and output laser.

The signal-to-SRS ratio for high-power delivery is determined by both the signal power and the initial Raman noise of the injected laser. In this experiment, although the laser source has an SRS-free spectrum at the highest power, the initial Raman noise is unknown. The SRS peak at the highest power in Fig. 4(a) may be caused by a high Raman noise at the input end. Note that spontaneous Raman noise varies with the characteristics of different light sources, hence the ultimate limit of high-power single-mode delivery should be considered dialectically. Since there is no effective method to detect the spontaneous Raman noise of the laser source at present, we try to explain the SRS dynamics in Fig. 4(a) by further simulation. Three fiber configurations, including

https://doi.org/10.1017/hpl.2024.91 Published online by Cambridge University Press

the uniform 24/200 μm profile (105 m), the uniform 48/400 μm profile (105 m), and the tapered fiber profile (105 m, similar to the fiber used in this work) are considered. The NA of three fibers is 0.06. The injected signal power is assumed to be 1000 W and the fiber attenuation is set to 3.5 dB/km.

Considering the Raman conversion in a long-distance delivery path, the power evolutions of signal laser and Stokes light are highly correlated to the injected Raman noise. Due to the high-fidelity delivery of single-mode laser in the experiment, it is reasonable to consider only the fundamental mode propagation. Then, the evolutions of signal and Stokes power versus the injected Raman noise are expressed by [37]:

$$\begin{cases} \dfrac{dP_s}{dz} = -\dfrac{\lambda_r}{\lambda_s}\dfrac{g_R}{A_{eff}(z)}P_sP_r - \alpha_s P_s \\ \dfrac{dP_r}{dz} = \dfrac{g_R}{A_{eff}(z)}P_rP_s - \alpha_r P_r \end{cases} \tag{3}$$

where P_s and P_r represent the signal power and Stokes power, and λ_s and λ_r represent the signal wavelength and Stokes wavelength. g_R is the Raman-gain coefficient, it is fixed to 6.43×10^{-14} W/m assuming that the polarization state is completely scrambled [38, 39]. α_s and α_r stand for background attenuation of two wavelengths. $A_{eff}(z)$ is defined as the effective interaction area at different locations. In the tapered fiber, A_{eff} changes with the fiber length and could be written as equation (4) at a specific location z:

$$A_{eff} = \frac{\iint I_s dS \iint I_r dS}{\iint I_s I_r dS} = \frac{\int_0^{2\pi}\int_0^{r_{clad}} \left|\vec{E}_s(r,\varphi)\right|^2 r dr d\varphi \cdot \int_0^{2\pi}\int_0^{r_{clad}} \left|\vec{E}_r(r,\varphi)\right|^2 r dr d\varphi}{\int_0^{2\pi}\int_0^{r_{clad}} \left|\vec{E}_s(r,\varphi)\right|^2 \left|\vec{E}_r(r,\varphi)\right|^2 r dr d\varphi} \tag{4}$$

https://doi.org/10.1017/hpl.2024.91 Published online by Cambridge University Press

where E and I represent the field and intensity distribution of fiber eigenmode. r and φ stand for the radial and angular coordinates, respectively.

Based on equations (3-4), the evolutions of signal and Stokes powers for three fiber configurations are calculated for comparison, the results are shown in Fig. 5. We set a principle of 50 dB to evaluate the laser delivery performance, i.e., a high-quality delivery is achieved if the final signal-to-SRS ratio is larger than 50 dB. It can be seen clearly in Fig. 5(a) that, when the Raman noise changes from 1×10^{-9} W to 1×10^{-6} W, the uniform 24/200 μm profile experiences a rapid decrement for the signal power due to the limited core mode area and a strong Raman conversion, accompanied by a sharp increment of Stokes power in Fig. 5(b). In this case, the signal-to-SRS ratio degrades from 38 dB to 10 dB (when the Raman noise is nearly 1×10^{-6} W) in Fig. 5(c), hence the long-distance delivery cannot be accomplished through the uniform 24/200 μm fiber directly. As for the uniform 48/400 μm fiber, the signal and Stokes power remain constant versus the varied Raman noise. Even with a larger Raman noise of 1×10^{-4} W, the signal-to-SRS ratio can reach nearly 50 dB, which enables a high-quality delivery. For the tapered multimode fiber, the performance of high-power delivery is improved greatly compared with the uniform 24/200 μm fiber and shows results close to that of uniform 48/400 μm fiber. This provides theoretical evidence of tapered multimode fiber for SRS-free delivery. Further, based on the experimental and simulated results, one can reasonably estimate that the Raman noise of the laser source employed in the experiment has a spontaneous Raman noise of nearly 2×10^{-6} W.

https://doi.org/10.1017/hpl.2024.91 Published online by Cambridge University Press

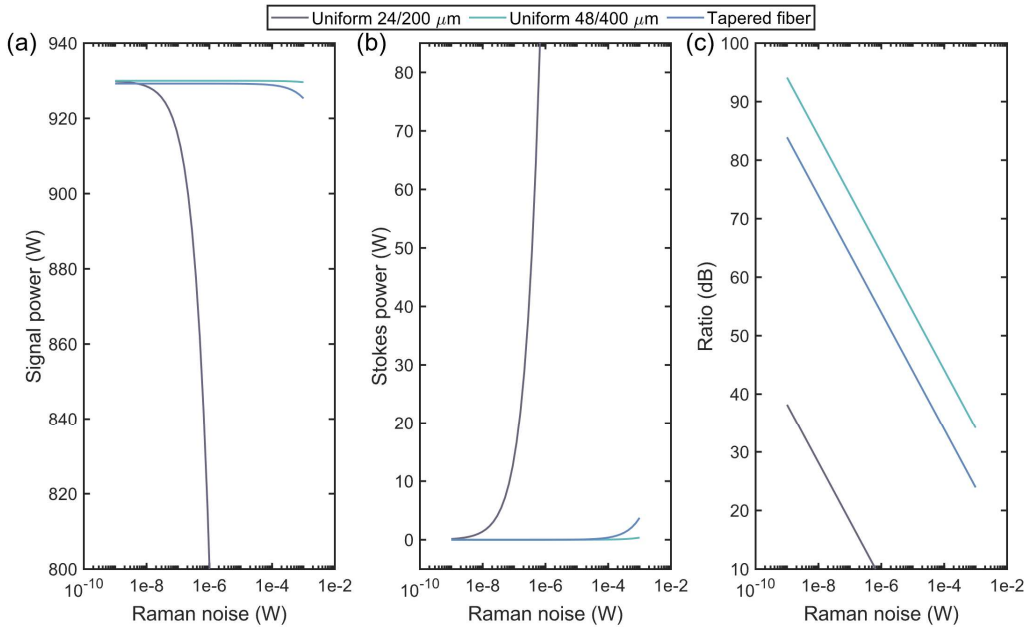

Fig. 5 The evolutions of (a) signal and (b) Stokes power versus the injected Raman noise, and (c) the corresponding signal-to-SRS ratios in uniform fibers or the tapered fiber.

The ultimate limits of the tapered multimode fiber for high-quality delivery are also investigated with different power levels. As illustrated in Fig. 6, the signal-to-SRS ratio decreases over 12 dB when the laser power increases from 1000 W to 2000 W. The principle (50 dB) of high-quality delivery restricts the injected Raman noise to 1.2×10^{-7} W. Hence, a laser source with a purer spectrum is needed to realize a high-quality delivery at 2000 W by using the fiber drawn in this work. When the laser power is 3000 W, the signal-to-SRS ratio remains below 50 dB for the whole range. In this way, an optimized design of the fiber profile, i.e., the core dimensions, tapered length, etc., should be conducted to improve the performance.

https://doi.org/10.1017/hpl.2024.91 Published online by Cambridge University Press

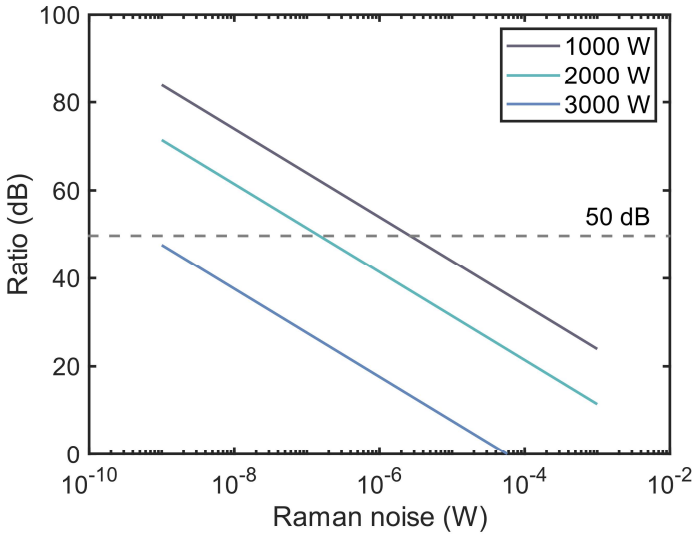

Fig. 6 The evolutions of signal-to-SRS ratios as a function of the injected Raman noise in the tapered multimode fiber with power levels of 1000 W, 2000 W and 3000 W laser.

Mode property is further characterized by using the spatially and spectrally resolved imaging technique [40] within the range of 1070 nm to 1090 nm, and the results are depicted in Fig. 7. In the whole delivery path, five kinds of HOMs are weakly excited due to the intrinsic defects of fiber structure. All the peak-to-peak amplitudes of them are measured to be below -30 dB. Insets show the phase and intensity distributions of five HOMs, suggesting the typical patterns of LP_{11}, LP_{21}, LP_{31}, LP_{12}, and LP_{41} modes, respectively. No radial HOMs ($LP_{0,N}$ modes, N = 1, 2, 3, …) are observed in the whole path, which reveals the adiabatic property of the tapered region. The unexpected excitation of azimuthal HOMs is mainly attributed to the slight fluctuation of fiber dimension since the actual fiber does not have theoretical uniformity. The mode preservation ensures the immunity of the delivery system for preventing beam quality degradation over a long distance.

https://doi.org/10.1017/hpl.2024.91 Published online by Cambridge University Press

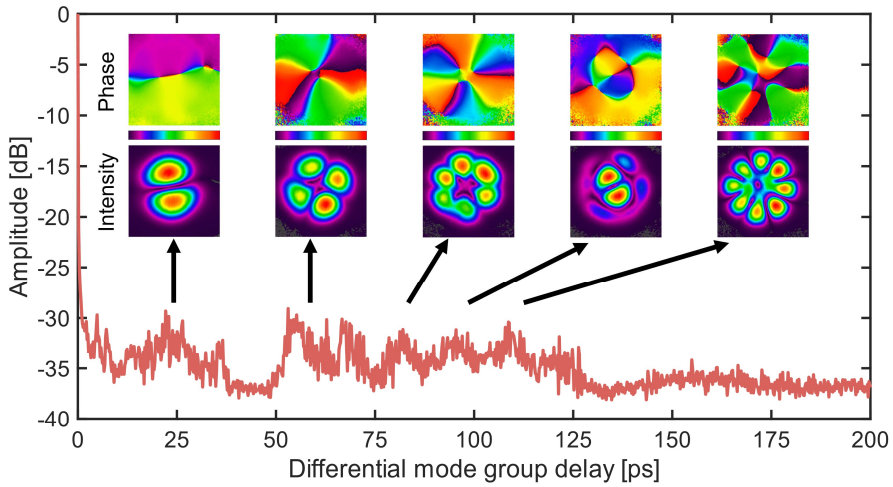

Fig. 7 Spatially and spectrally resolved imaging results for the whole delivery path.

With a weakly coupled regime, the current results of M^2 factor and mode diagnosis demonstrate the convenience of high-fidelity delivery. To achieve this goal, a key premise is controlling the launching condition. Once the laser modes are coupled into the deliver fiber with high fidelity, the weakly coupled regime can keep the field contents intact.

IV. DISCUSSION: ULTIMATE LIMITS FOR HIGH-POWER, SINGLE-MODE, AND LONG-DISTANCE DELIVERY BASED ON SOLID-CORE FIBERS

As high-power laser delivery becomes a reawakened subject, many power records have been generated for long-distance and single-mode transmission in recent years. To pursue the bilateral limits for power and delivery length, the transmission characteristics with different presupposed parameters should be further discussed. Considering the difference of laser sources in terms of Raman noise, it is not meaningful to estimate the SRS threshold directly by the simplified formula $P_{th} \approx 16 A_{eff} / (g_R \cdot L)$, in

https://doi.org/10.1017/hpl.2024.91 Published online by Cambridge University Press

which A_{eff}, g_R, and L represent the effective mode area, Raman-gain coefficient, and fiber length, respectively. The final signal-to-stokes ratio is affected by laser power, Raman noise, fiber parameters, and delivery length synchronously.

Based on the weakly coupled condition and the fiber parameters used in this work, the further discussion here assumes the core diameter to 48 μm, and the NA is 0.06. For simplicity and universality, the uniform fiber profile is selected for reference. The transmission attenuation at 1080 nm is set to 5 dB/km. This is a moderate value of attenuation for current passive laser fibers. In all the simulations, an ideal single-mode beam is adopted, since the experiment described in this work has verified the inherent advantage of a tapered fiber scheme for high-fidelity delivery, and this technique can be widely extended. The simulations also obey the power evolution equation (3).

Figure 8 displays the relationships between the initial Raman noise and the output properties with different fiber lengths and an injected signal power of 1000 W. For the delivery length of 100 m, the output signal power keeps a stable value of nearly 935 W. Even with a large Raman noise, e.g., 1×10^{-3} W, the Stokes power does not increase significantly, and the signal-to-Stokes ratio is estimated to be higher than 35 dB. If we set a signal-to-Stokes ratio of 50 dB as the principle for high-quality delivery, the initial Raman noise power of the laser source should be maintained in the order of 10^{-4} W or lower values when the delivery length is 100 m. As the delivery length extends to 150 m, a stronger Raman conversion is observed. At the maximum Raman noise, the conversion of signal light and Stokes light experiences a significant increment, resulting in a signal-to-Stokes ratio of less than -30 dB at the output end. According to the

https://doi.org/10.1017/hpl.2024.91 Published online by Cambridge University Press

calculation results, it is a challenging task to obtain a high-quality delivery of 175 m or 200 m for a 1000 W single-mode laser. To achieve these goals, the Raman noises of the laser source should be controlled to below the orders of 1×10^{-6} W and 1×10^{-7} W, respectively.

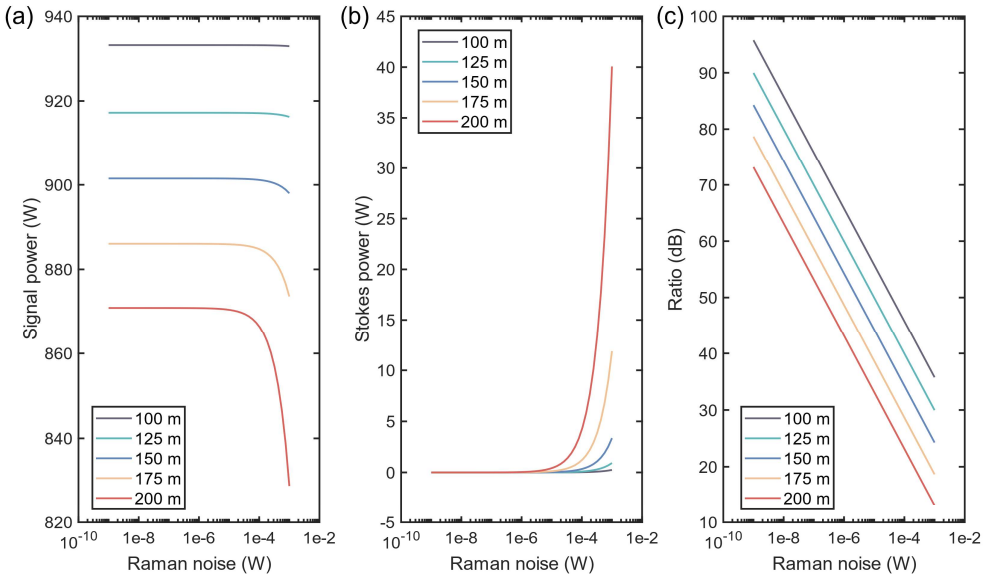

Fig. 8 Relationships between the initial Raman noise and the output properties with different fiber lengths and an injected signal power of 1000 W. (a) Output signal power, (b) output Stokes power, and (c) output signal-to-Stokes ratio.

Similarly, Figure 9 displays the relationships between the initial Raman noise and the output properties with different fiber lengths and an injected signal power of 2000 W. When the delivery length is 50 m, the signal-to-Stokes ratio keeps over 40 dB if the Raman noise varies from 1×10^{-9} W and 1×10^{-3} W. To realize a signal-to-Stokes ratio over 50 dB, the power level of Raman noise should be less than the order of 1×10^{-4} W, meaning that the 2 kW laser source should have an initial signal-to-SRS ratio larger than 73 dB. Consequently, the demand for high-power, single-mode laser delivery puts

https://doi.org/10.1017/hpl.2024.91 Published online by Cambridge University Press

forward higher requirements on developing laser sources with high spectral purity. When the delivery length is 75 m, a high-quality delivery restricts the Raman noise to nearly the order of 1×10^{-5} W, in this case, the initial signal-to-SRS ratio of the laser source is over 83 dB. When the delivery length is 100 m, an obvious Raman conversion could be seen if the Raman noise is larger than 1×10^{-6} W, which degrades the transmission efficiency and spectral purity. In a word, based on the solid-core fibers of below 50 μm, it is a tough target to achieve a delivery length of over 100 m at the power level of 2000 W.

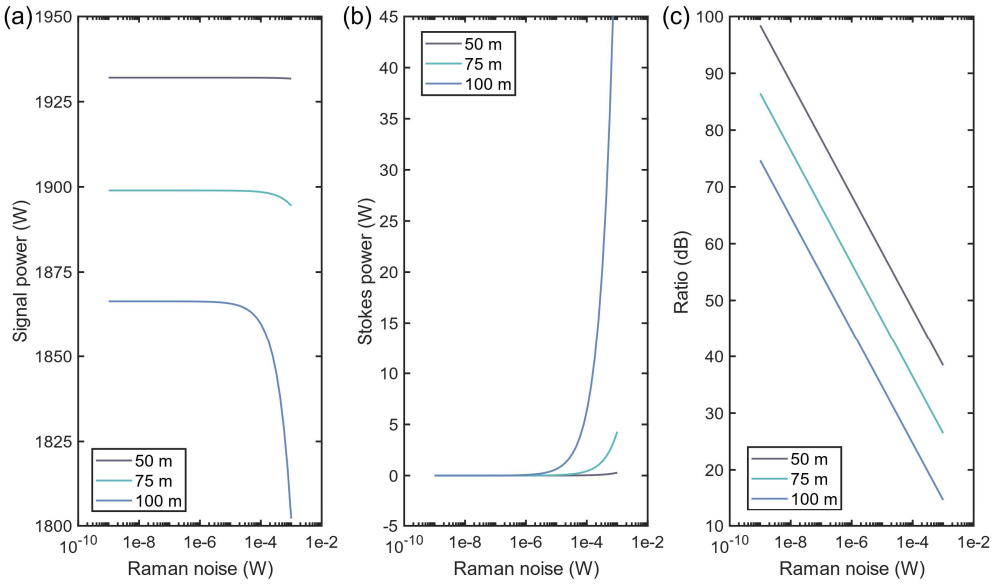

Fig. 9 Relationships between the initial Raman noise and the output properties with different fiber lengths and an injected signal power of 2000 W. (a) Output signal power, (b) output Stokes power, and (c) output signal-to-Stokes ratio.

To determine the ultimate limits of high-power delivery, the cases for 3000 W are also calculated, as shown in Fig. 10 (a-c). When the Raman noise is 1×10^{-4} W, the signal-to-Stokes ratios for 50 m, 75 m, and 100 m delivery lengths are 38 dB, 20 dB,

https://doi.org/10.1017/hpl.2024.91 Published online by Cambridge University Press

and 2.3 dB, respectively. When the Raman noise is 1×10^{-5} W, the signal-to-Stokes ratios for 50 m, 75 m, and 100 m delivery lengths are 48 dB, 30 dB, and 12 dB, respectively. When the Raman noise is 1×10^{-6} W, the signal-to-Stokes ratios for 50 m, 75 m, and 100 m delivery lengths are 57 dB, 39 dB, and 22 dB, respectively. When the Raman noise is 1×10^{-7} W, the signal-to-Stokes ratios for 50 m, 75 m, and 100 m delivery lengths are 68 dB, 50 dB, and 32 dB, respectively. As for the delivery length of 100 m, the requirement on Raman noise is lower than 1×10^{-9} W if a signal-to-Stokes ratio of over 50 dB is expected.

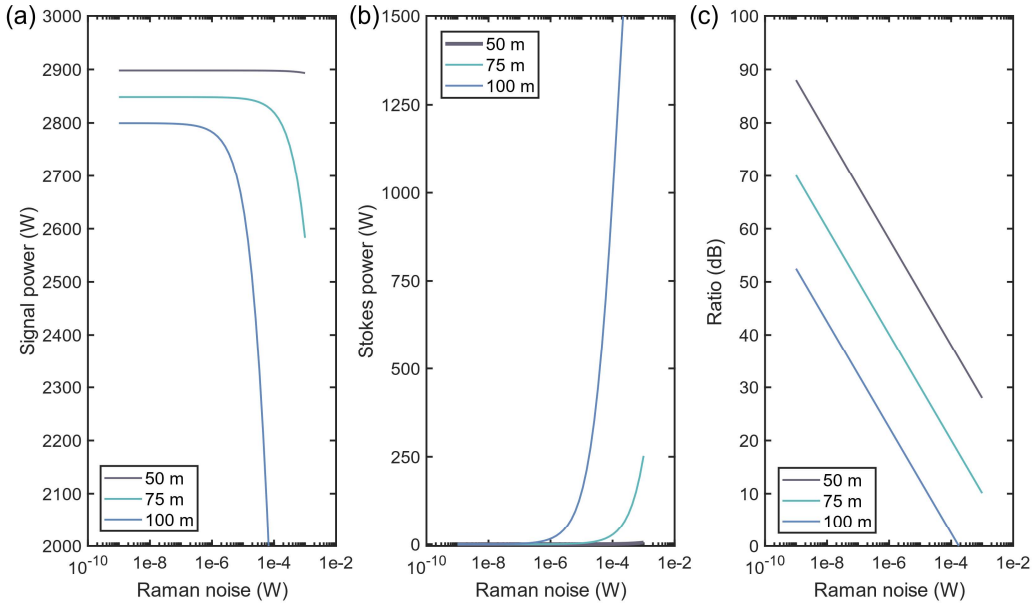

Fig. 10 Relationships between the initial Raman noise and the output properties with different fiber lengths and an injected signal power of 3000 W. (a) Output signal power, (b) output Stokes power, and (c) output signal-to-Stokes ratio.

V. CONCLUSION

The current work provides a successful scheme to balance the nonlinear effects and beam quality degradation for the long-distance delivery of high-power single-mode

https://doi.org/10.1017/hpl.2024.91 Published online by Cambridge University Press

laser. Here, we experimentally realize a kilowatt-level delivery of 105 m enabled by a tapered multimode fiber. With the maximum input power of 1035 W, the maximum output power is 962 W, corresponding to a high efficiency of over 93% and a high signal-to-SRS ratio of over 50 dB. The tapered multimode fiber is carefully designed with the weakly coupled condition and adiabatically drawn from a thin end of 24/200 μm to a thick end of 48/400 μm. Due to the excellent taper profile and the optimum excitation at the input end, a high-fidelity delivery without beam deterioration is demonstrated, which results in M^2 factors of 1.20 and 1.23 for the input and output lasers, respectively. The mode property resolved by the mode imaging technique shows slight HOM contents of less than -30 dB in the whole delivery path, which further supports the evidence of high-fidelity transmission.

To observe the ultimate limits for high-power laser delivery, the output properties of 48 μm fibers with different delivery lengths and laser powers are calculated as a function of the injected Raman noise. We set a high signal-to-Stokes ratio of 50 dB to evaluate a high-quality delivery. Results show that, for solid-core fibers below 50 μm, it is a challenging task to obtain a high-quality delivery of 175 m or 200 m for a 1000 W single-mode laser unless the Raman noises of the laser source are controlled to below the orders of 1×10^{-6} W or 1×10^{-7} W, respectively. Similarly, a delivery length of over 100 m at the power level of 2000 W restricts the Raman noise to be lower than the order of 1×10^{-6} W. When the laser power is 3000 W, the different orders of Raman noise, i.e., 1×10^{-6} W, 1×10^{-7} W, 1×10^{-9} W, determine the ultimate delivery lengths to 50 m, 75 m, and 100 m, respectively.

https://doi.org/10.1017/hpl.2024.91 Published online by Cambridge University Press

In addition, the scheme of tapered delivery fiber can be easily combined with the functional schemes. Since the tapered fiber modulates the light transmission along the longitudinal direction, it is a promising way to incorporate it with the transverse designs, including the designs with stronger high-order mode suppression, and weaker light-acoustics interaction, etc.

Acknowledgement

This work is supported by the National Key R&D Program of China (2022YFB3606000) and the Graduate Innovation Project of Hunan Province (QL20220004).

References

1. H. C. H. Mulvad, S. Abokhamis Mousavi, V. Zuba, L. Xu, H. Sakr, T. D. Bradley, J. R. Hayes, G. T. Jasion, E. Numkam Fokoua, A. Taranta, S. U. Alam, D. J. Richardson, and F. Poletti, "Kilowatt-average-power single-mode laser light transmission over kilometre-scale hollow-core fibre," Nature Photonics **16**, 448-453 (2022).
2. J. Yao, X. Zhang, B. Li, B. Wang, D. Jin, Y. Duan, J. Zhao, and P. Wang, "High-efficiency distortion-free delivery of 3 kW continuous-wave laser using low-loss multi-mode nested hollow-core anti-resonant fiber," Journal of Lightwave Technology, 1-8 (2024).
3. M. A. Cooper, J. Wahlen, S. Yerolatsitis, D. Cruz-Delgado, D. Parra, B. Tanner, P. Ahmadi, O. Jones, M. S. Habib, I. Divliansky, J. E. Antonio-Lopez, A. Schülzgen, and R. Amezcua Correa, "2.2 kW single-mode narrow-linewidth laser delivery through a hollow-core fiber," Optica **10**, 1253-1259 (2023).

4. C. Rohrer, C. A. Codemard, G. Kleem, T. Graf, and M. A. Ahmed, "Preserving Nearly Diffraction-Limited Beam Quality Over Several Hundred Meters of Transmission Through Highly Multimode Fibers," Journal of Lightwave Technology **37**, 4260-4267 (2019).
5. C. N. Danson, C. Haefner, J. Bromage, T. Butcher, J.-C. F. Chanteloup, E. A. Chowdhury, A. Galvanauskas, L. A. Gizzi, J. Hein, D. I. Hillier, N. W. Hopps, Y. Kato, E. A. Khazanov, R. Kodama, G. Korn, R. Li, Y. Li, J. Limpert, J. Ma, C. H. Nam, D. Neely, D. Papadopoulos, R. R. Penman, L. Qian, J. J. Rocca, A. A. Shaykin, C. W. Siders, C. Spindloe, S. Szatmári, R. M. G. M. Trines, J. Zhu, P. Zhu, and J. D. Zuegel, "Petawatt and exawatt class lasers worldwide," High Power Laser Science and Engineering **7**, 03000e03054 (2019).
6. J. Zuo and X. Lin, "High-Power Laser Systems," Laser & Photonics Reviews **16**, 2100741 (2022).
7. W. Shi, Q. Fang, X. s. Zhu, R. A. Norwood, and N. Peyghambarian, "Fiber lasers and their applications [Invited]," Appl. Opt. **53**, 6554-6568 (2014).
8. C. Jauregui, J. Limpert, and A. Tünnermann, "High-power fibre lasers," Nature Photonics **7**, 861-867 (2013).
9. M. O'Connor, V. Gapontsev, V. Fomin, M. Abramov, and A. Ferin, "Power Scaling of SM Fiber Lasers toward 10kW," in Conference on Lasers and Electro-Optics/International Quantum Electronics Conference, OSA Technical Digest (CD) (Optica Publishing Group, 2009), paper CThA3.
10. S. Kensuke, I. Shinya, U. Keisuke, T. Yuya, K. Masahiro, and T. Daiichiro, "5-kW single stage all-fiber Yb-doped single-mode fiber laser for materials processing," Proc. SPIE 10512, Fiber Lasers XV: Technology and Systems, 105120C .
11. X. Chen, T. Yao, L. Huang, Y. An, H. Wu, Z. Pan, and P. Zhou, "Functional Fibers and Functional Fiber-Based Components for High-Power Lasers," Advanced Fiber Materials **5**, 59-106 (2023).

https://doi.org/10.1017/hpl.2024.91 Published online by Cambridge University Press

12. H. Wu, X. Chen, L. Huang, and P. Zhou, "9 - Specialty optical fiber for high-average-power laser operation," in *Specialty Optical Fibers*, M. F. S. Ferreira and M. C. Paul, eds. (Woodhead Publishing, 2024), pp. 207-230.
13. X. Zhang, S. F. Gao, Y. Y. Wang, W. Ding, and P. Wang, "Design of large mode area all-solid anti-resonant fiber for high-power lasers," High Power Laser Science and Engineering **9** (2021).
14. D. Jain, Y. Jung, M. Nunez-Velazquez, and J. K. Sahu, "Extending single mode performance of all-solid large-mode-area single trench fiber," Opt. Express **22**, 31078-31091 (2014).
15. Y. An, H. Yang, X. Chen, L. Huang, Z. Yan, Z. Pan, Z. Wang, Z. Jiang, and P. Zhou, "Seeing the strong suppression of higher order modes in single trench fiber using the S^2 technique," Opt. Lett. **48**, 61-64 (2023).
16. S. Hochheim, E. Brockmüller, P. Wessels, M. Steinke, J. Koponen, T. Lowder, S. Novotny, J. Neumann, and D. Kracht, "Highly-Integrated Signal and Pump Combiner in Chirally-Coupled-Core Fibers," Journal of Lightwave Technology **39**, 7246-7250 (2021).
17. X. Chen, L. Huang, H. Yang, X. Xi, Y. An, Z. Yan, Y. Chen, Z. Pan, and P. Zhou, "Large-mode-area multi-resonant all-solid photonic bandgap fiber with low bending loss and robust single-mode operation," Optics & Laser Technology **157**, 108668 (2023).
18. H. Li, C. Goel, J. Zang, S. Raghuraman, S. Chen, M. R. Abu Hassan, W. Chang, and S. Yoo, "Integration of an anti-resonant hollow-core fiber with a multimode Yb-doped fiber for high power near-diffraction-limited laser operation," Opt. Express **30**, 7928-7937 (2022).
19. T. Matsui, K. Tsujikawa, T. Okuda, N. Hanzawa, Y. Sagae, K. Nakajima, Y. Fujiya, and K. Shiraki, "Effective Area Enlarged Photonic Crystal Fiber with Quasi-Uniform Air-Hole Structure for High Power Transmission," IEICE Transactions on Communications **E103.B**, 415-421 (2020).

https://doi.org/10.1017/hpl.2024.91 Published online by Cambridge University Press

20. X. Zhu, D. Wu, Y. Wang, F. Yu, Q. Li, Y. Qi, J. Knight, S. Chen, and L. Hu, "Delivery of CW laser power up to 300 watts at 1080nm by an uncooled low-loss anti-resonant hollow-core fiber," Opt. Express **29**, 1492-1501 (2021).

21. D. Wu, F. Yu, C. Wu, M. Zhao, J. Zheng, L. Hu, and J. Knight, "Low-loss multi-mode anti-resonant hollow-core fibers," Opt. Express **31**, 21870-21880 (2023).

22. H. Sakr, Y. Chen, G. T. Jasion, T. D. Bradley, J. R. Hayes, H. C. H. Mulvad, I. A. Davidson, E. Numkam Fokoua, and F. Poletti, "Hollow core optical fibres with comparable attenuation to silica fibres between 600 and 1100 nm," Nature Communications **11**, 6030 (2020).

23. S. Gao, Y. Wang, W. Ding, D. Jiang, S. Gu, X. Zhang, and P. Wang, "Hollow-core conjoined-tube negative-curvature fibre with ultralow loss," Nature Communications **9**, 2828 (2018).

24. Q. Fu, Y. Wu, I. A. Davidson, L. Xu, G. T. Jasion, S. Liang, S. Rikimi, F. Poletti, N. V. Wheeler, and D. J. Richardson, "Hundred-meter-scale, kilowatt peak-power, near-diffraction-limited, mid-infrared pulse delivery via the low-loss hollow-core fiber," Opt. Lett. **47**, 5301-5304 (2022).

25. Q. Fu, I. A. Davidson, S. M. A. Mousavi, H. C. H. Mulvad, N. V. Wheeler, L. Xu, F. Poletti, and D. J. Richardson, "Hollow-Core Fiber: Breaking the Nonlinearity Limits of Silica Fiber in Long-Distance Green Laser Pulse Delivery," Laser & Photonics Reviews **18**, 2201027 (2024).

26. S. Jiang, L. Ma, Z. Zhang, X. Xu, S. Wang, J. Du, C. Yang, W. Tong, and Z. He, "Design and Characterization of Ring-Assisted Few-Mode Fibers for Weakly Coupled Mode-Division Multiplexing Transmission," Journal of Lightwave Technology **36**, 5547-5555 (2018).

27. M. Fermann, "Single-mode excitation of multimode fibers with ultrashort pulses," Opt. Lett. **23**, 52-54 (1998).

28. S. Hurand, L.-A. Chauny, H. El-Rabii, S. Joshi, and A. Yalin, "Mode coupling and output beam quality of 100–400 μm core silica fibers," Appl. Opt. **50**, 492-499 (2011).

https://doi.org/10.1017/hpl.2024.91 Published online by Cambridge University Press

29. A. P. Yalin, "High power fiber delivery for laser ignition applications," Opt. Express **21**, A1102-A1112 (2013).

30. L. Bansal, R. Sienkowski, C. Neale, J. Mann, and J. W. Nicholson, "S^2 mode content measurement of a 7+1 to 1 backward pump-signal combiner," Proc. SPIE 12866, Components and Packaging for Laser Systems X, 1286604 (12 March 2024).

31. X. Chen, S. Huang, L. Huang, L. Du, Z. Yan, Z. Pan, P. Zhou, and Z. Jiang, "Tracing the origins of mode coupling for beam quality optimization in high-power fiber laser delivery system," High Power Laser Science and Engineering, **in Early Posting** (2024).

32. D. Marcuse, *Theory of dielectric optical waveguides* (Elsevier, 2013).

33. J. M. Fini, "Intuitive modeling of bend distortion in large-mode-area fibers," Opt. Lett. **32**, 1632-1634 (2007).

34. J. M. Fini and S. Ramachandran, "Natural bend-distortion immunity of higher-order-mode large-mode-area fibers," Opt. Lett. **32**, 748-750 (2007).

35. M.-J. Li, X. Chen, A. Liu, S. Gray, J. Wang, D. T. Walton, and L. A. Zenteno, "Limit of Effective Area for Single-Mode Operation in Step-Index Large Mode Area Laser Fibers," Journal of Lightwave Technology **27**, 3010-3016 (2009).

36. S. Vincenzo, A. C. Christophe, D. Mike, and N. Z. Michalis, "Splice optimisation between dissimilar fibres in the presence of dopant diffusion," Proc. SPIE 12865, Fiber Lasers XXI: Technology and Systems, 1286515 (12 March 2024).

37. J. Ji, C. A. Codemard, M. Ibsen, J. K. Sahu, and J. Nilsson, "Analysis of the Conversion to the First Stokes in Cladding-Pumped Fiber Raman Amplifiers," IEEE Journal of Selected Topics in Quantum Electronics **15**, 129-139 (2009).

38. G. P. Agrawal, "Nonlinear Fiber Optics," in *Nonlinear Science at the Dawn of the 21st Century*, (Springer Berlin Heidelberg, 2000), 195-211.

39. S. T. Davey, D. L. Williams, B. J. Ainslie, W. J. M. Rothwell, and B. Wakefield, "Optical gain spectrum of GeO_2-SiO_2 Raman fibre amplifiers," in *IEE Proceedings J (Optoelectronics),* (1989), pp. 301-306.

https://doi.org/10.1017/hpl.2024.91 Published online by Cambridge University Press

40. J. W. Nicholson, A. D. Yablon, J. M. Fini, and M. D. Mermelstein, "Measuring the Modal Content of Large-Mode-Area Fibers," IEEE Journal of Selected Topics in Quantum Electronics **15**, 61-70 (2009).

https://doi.org/10.1017/hpl.2024.91 Published online by Cambridge University Press